VIP Lithium–Sulfur Batteries Very Important Paper

International Edition: DOI: 10.1002/anie.201511553
German Edition: DOI: 10.1002/ange.201511553

Elemental-Sulfur-Mediated Facile Synthesis of a Covalent Triazine Framework for High-Performance Lithium–Sulfur Batteries

Siddulu Naidu Talapaneni[+], Tae Hoon Hwang[+], Sang Hyun Je, Onur Buyukcakir, Jang Wook Choi, and Ali Coskun**

Abstract: *A covalent triazine framework (CTF) with embedded polymeric sulfur and a high sulfur content of 62 wt % was synthesized under catalyst- and solvent-free reaction conditions from 1,4-dicyanobenzene and elemental sulfur. Our synthetic approach introduces a new way of preparing CTFs under environmentally benign conditions by the direct utilization of elemental sulfur. The homogeneous sulfur distribution is due to the in situ formation of the framework structure, and chemical sulfur impregnation within the micropores of CTF effectively suppresses the dissolution of polysulfides into the electrolyte. Furthermore, the triazine framework facilitates electron and ion transport, which leads to a high-performance lithium–sulfur battery.*

Sulfur is one of the most abundant elements, and more than 70 million tons of elemental sulfur are annually produced as a by-product of the hydrodesulfurization process in the petroleum refining industry. This mostly involuntary production of sulfur, however, creates a significant global supply surplus. Therefore, the development of highly functional sulfur-rich polymers that are synthesized by the direct utilization of elemental sulfur can be a useful direction for recycling the abundant sulfur to synthesize value-added products. Rechargeable lithium–sulfur (Li–S) batteries have received significant attention in recent years as one such possibility owing to their high theoretical gravimetric capacity and energy density of 1675 $mAh\,g^{-1}$ and 2567 $Wh\,kg^{-1}$, respectively.[1] However, despite almost 30 years of development, Li–S batteries are still at the research stage because of insufficient cycle lifetimes, which mainly arise from the fatal redox shuttling process that is due to the dissolution of the intermediate lithium polysulfide species into most of the currently used organic electrolytes during the charge/discharge process.[2] One of the most widely adopted approaches to address this issue is the physical encapsulation of elemental sulfur within porous conductive media, such as ordered mesoporous carbon (CMK-3).[3] The use of these conductive media also supplements the intrinsically low conductivity of sulfur by providing fast electron pathways.[3] Other conductive media, such as hierarchical porous carbon (HPC),[4] carbon nanotubes,[5] porous carbon fibers,[6] graphene,[7] conducting polymers,[8] pyrolyzed polyacrylonitrile,[6,9] and metal oxides,[10] have also been investigated. Although these approaches have improved the cycling performance to large extents, these architectures and polymer coatings still suffer from a certain possibility of polysulfide dissolution, because complete encapsulation during repeated charge–discharge cycles is technically infeasible.[11] In a similar sense, the negligible binding of sulfur within the matrices also prevents the complete elimination of polysulfide dissolution. To overcome this limitation, the impregnation of sulfur through the formation of strong covalent bonds between carbon and sulfur has been explored.[9c,12] Recently, Pyun and co-workers[12] developed an innovative strategy of "inverse vulcanization" to prepare polymers with a high sulfur content directly from elemental sulfur for their use as active cathode materials in Li–S batteries. More recently, Park et al.[13] prepared triazine-based 3D-interconnected sulfur-rich polymers, in which the triazine units are linked by sulfur chains. These approaches are undoubtedly promising examples for the development of superior sulfur cathodes. However, the poor conductivity of sulfur-containing polymers still appears to be a fundamental challenge. More critically, irregular sulfur domains linked by small organic molecules leave a certain amount of sulfur unbound to the polymer matrices after prolonged cycling, because lithiation cleaves S–S bonds in sulfur chains. These cleaved bonds may not recover their original state during the subsequent delithiation and thereafter, giving rise to some isolated sulfur domains, particularly when the initial sulfur domains are scattered and have irregular sizes. These unbound sulfur domains are vulnerable to dissolution into the electrolyte upon formation of soluble polysulfides, as observed with the aforementioned encapsulated cases. Therefore, it is desirable to develop a framework structure that features 1) robust sulfur binding, 2) an ordered pore structure for regular sulfur distribution, 3) large void spaces for high sulfur loadings, and 4) good electronic/ionic conductivity.

Covalent triazine frameworks (CTFs) are a class of microporous polymers with narrow pore-size distributions and extremely high specific surface areas (up to 3000 $m^2\,g^{-1}$) along with a moderate conductivity. Antonietti, Thomas, and co-workers first reported the synthesis of CTFs through

[*] Dr. S. N. Talapaneni,[+] T. H. Hwang,[+] S. H. Je, Dr. O. Buyukcakir, Prof. J. W. Choi, Prof. A. Coskun
Graduated School of EEWS and KAIST Institute Nano Century
Korea Advanced Institute of Science and Technology (KAIST)
Daejeon, 305-701 (Korea)
E-mail: jangwookchoi@kaist.ac.kr
coskun@kaist.ac.kr
Prof. A. Coskun
Department of Chemistry
Korea Advanced Institute of Science and Technology (KAIST)
Daejeon, 305-701 (Korea)
[+] These authors contributed equally to this work.
Supporting information and ORCID(s) from the author(s) for this article are available on the WWW under http://dx.doi.org/10.1002/anie.201511553.

ionothermal synthesis using molten $ZnCl_2$ as both the solvent and catalyst for the cyclotrimerization of aromatic nitriles at relatively high temperatures (400–700 °C).[14] Since their discovery, CTFs have been exploited in a wide range of applications, including heterogeneous catalysis, metal-free CO_2 activation, photocatalysis, gas storage, adsorption of toxic organic compounds, hydrocarbon separation, electrochemical double-layer supercapacitors, lithium storage, and lithium batteries, as electrocatalysts, solid supports for metal nanoparticles in catalysis, and gas sensors.[15] Recently, the groups of Dai and Cooper[16] reported the synthesis of CTFs with biphenyl- and triphenyl-spaced nitriles using trifluoromethanesulfonic acid as the catalyst both at room temperature and under microwave-assisted conditions with the aim of preparing CTFs without any residual inorganic contamination (often mainly metallic $ZnCl_2$). However, the preparation of CTF-1 with trifluoromethanesulfonic acid as the catalyst is infeasible, mainly because of the structural rigidity of the monomer 1,4-dicyanobenzene.[16b]

Herein, we report the sulfur-mediated synthesis of CTF-1 (S-CTF-1) from 1,4-dicyanobenzene and elemental sulfur without any catalysts or solvents (Scheme 1). The formation of CTF proceeds by in situ vulcanization with elemental sulfur, enabling both the covalent attachment of sulfur and its homogeneous distribution within the pores. S-CTF-1 was found to have a high sulfur content of 62 wt% along with a well-shaped bipyramidal morphology, which was been achieved without the use of any external templates. We have also examined the electrochemical performance of S-CTF-1 as a sulfur cathode material in Li–S batteries. S-CTF-1 exhibited a robust cycling performance for 300 cycles with 85.8% capacity retention along with the highest initial Coulombic efficiency (ICE) reported to date: 94.4% at 0.05 C (25 mA g^{-1}).

The synthesis of S-CTF-1 was achieved by the cyclotrimerization of 1,4-dicyanobenzene in elemental sulfur at 400 °C to promote efficient ring opening of elemental sulfur and to activate the cyano groups for the cyclization reaction (see the Supporting Information for details). We applied

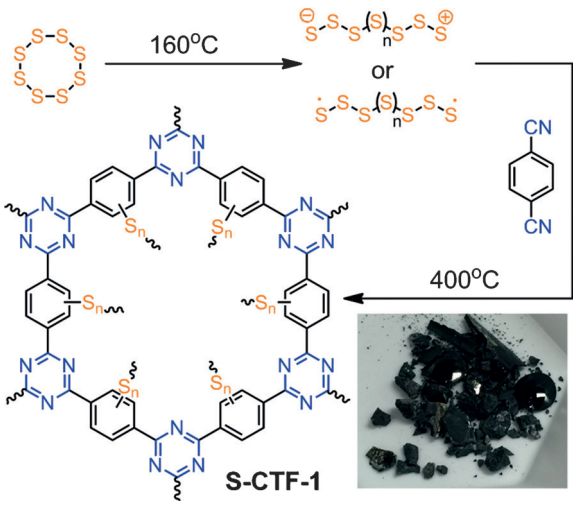

Scheme 1. Synthesis of S-CTF-1 from elemental sulfur and an optical image of S-CTF-1.

a stepwise heating process, first to 160 °C to dissolve the elemental sulfur and then to 400 °C to initiate the ring-opening polymerization of elemental sulfur into a linear polysulfane, which promotes the trimerization of the nitrile groups, while the singlet state of sulfur can undergo C–H insertion reactions for the simultaneous chemical sulfur impregnation of CTF-1. It is noteworthy that simultaneous framework formation and sulfur polymerization/insertion led to a homogeneous distribution of sulfur within the micropores. This process was accompanied (Scheme 1) by a significant color change from pale yellow to black (Scheme 1, inset), which indicates graphitization of the framework. To investigate the textural properties of S-CTF-1, we also carried out Brunauer–Emmett–Teller (BET) analysis. S-CTF-1 was found to be non-porous, pointing to the fact that the original pores of CTF-1 were fully occupied by sulfur.

To evaluate the crystallinity of S-CTF-1, it was analyzed by powder X-ray diffraction (PXRD) analysis (see the Supporting Information, Figure S1). Whereas S-CTF-1 was found to be mostly amorphous, some crystalline elemental sulfur peaks remained in the PXRD spectrum of S-CTF-1, implying that some elemental sulfur was physically trapped and crystallized within the framework even after the heat treatment at 400 °C. Evidently, the XRD pattern of the trapped sulfur is in good agreement with that of crystalline sulfur.[17] To further confirm the formation of S-CTF-1, Fourier transform infrared spectroscopy (FT-IR) analysis was conducted (Figure S2). The disappearance of the characteristic nitrile stretching band at 2218 cm^{-1} verified the complete cyclization of 1,4-dicyanobenzene to form the corresponding triazine ring. Moreover, the appearance of the characteristic absorption bands at 1500–1700 cm^{-1} further confirmed the successful formation of triazine rings.[14] The C–S and S–S stretching bands at 750 and 550–600 cm^{-1} indicated the formation of C–S bonds and polymeric sulfane within the framework.

Elemental analysis (EA) and X-ray photoelectron spectroscopy (XPS) survey spectra reveal that S-CTF-1 mainly consists of sulfur, carbon, and nitrogen with a small amount of hydrogen. XPS analysis of S-CTF-1 gave a composition of 62 wt% sulfur, 33 wt% carbon, and 4 wt% nitrogen (Figure 1 a), which is in good agreement with the EA data (see the Supporting Information). The nature of the chemical bonding in S-CTF-1 was further investigated by XPS analysis. The XPS survey analysis, which revealed the presence of only sulfur, carbon, and nitrogen in S-CTF-1, indicates that S-CTF-1 is of high purity. The XPS C 1s spectrum could be deconvoluted (Figure 1 b) into three peaks with binding energies of 284.6, 286.2, and 286.8 eV. The lowest-energy contribution of 284.6 eV can be assigned to the carbon atoms of the aryl rings present in the CTF framework and also to the adventitious carbon (C–C) used for calibration.[15d] The peak at 286.2 eV was associated with C–S bonding, further confirming the formation of covalent C–S bonds within S-CTF-1.[18] The third peak at 286.8 eV was assigned to the carbon atoms present in the triazine (N=C–N) ring. The XPS N core-level 1s spectrum of S-CTF-1 (Figure 1 c) is in perfect agreement with those previously reported for CTFs, showing a dominant single peak at around 399 eV, which was assigned

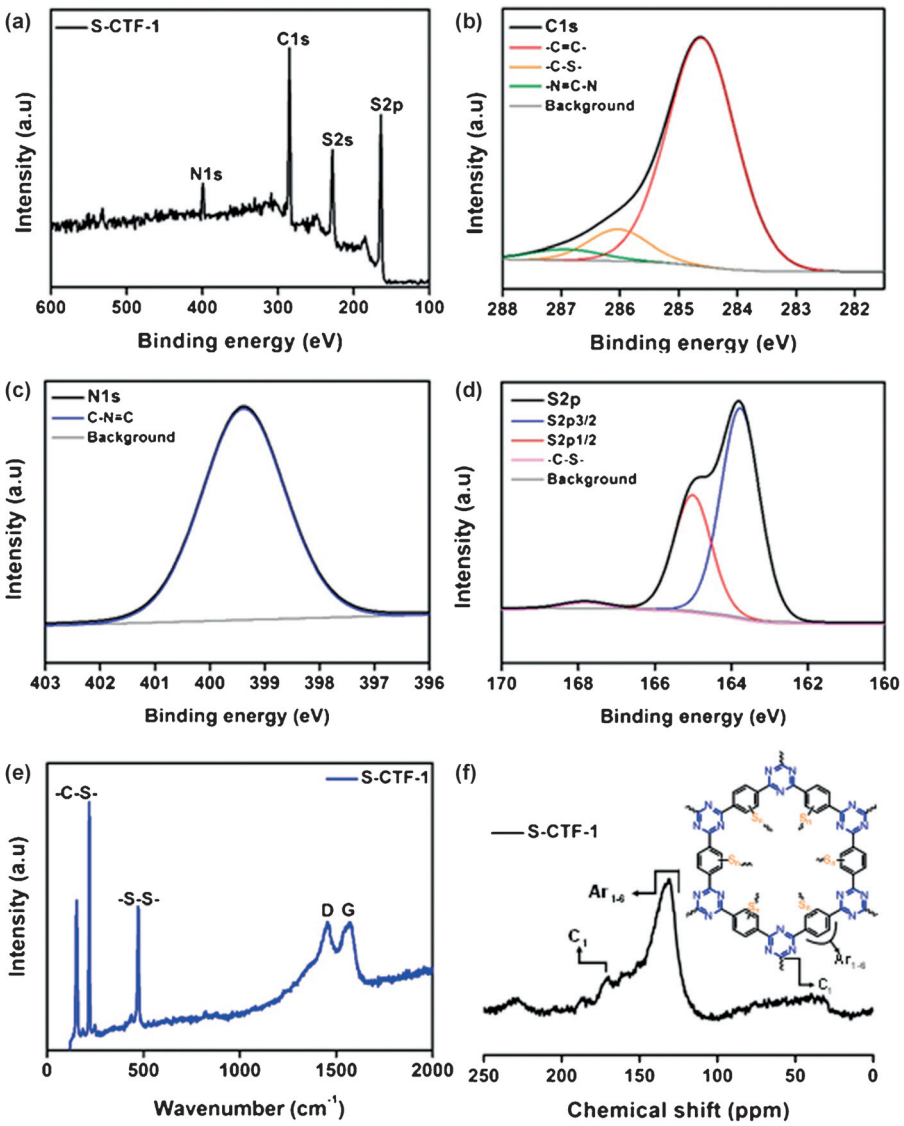

Figure 1. a–d) XPS survey, C 1s, N 1s, and S 2p spectra of S-CTF-1. e, f) Raman and ^{13}C NMR CP/MAS spectra of S-CTF-1.

to the nitrogen atoms within the triazine units (C–N=C).[15d,19] The high-resolution S 2p XPS spectrum contained three major peaks with binding energies of 163.7, 164.8, and 168.4 eV (Figure 1c). The former two peaks can be attributed to the S $2p_{3/2}$ and the S $2p_{1/2}$ states of the $-C-S_n-C-$ chain (n = 5–6),[18,20] whereas the smallest peak at 168.4 eV corresponds to C–S groups,[18b,20] confirming that sulfur was successfully incorporated into the CTF-1 structure. To further confirm the formation of CTF-1, the sample was characterized by Raman spectroscopy, which revealed the presence of D and G bands at 1450 and 1565 cm^{-1} (Figure 1e). A deviation in the D and G bands of S-CTF-1 was observed compared to that of a CTF-1 sample that was synthesized using $ZnCl_2$ as the catalyst and reaction medium (1360 and 1600 cm^{-1}).[15e] This difference can be attributed to the presence of elemental/polymeric sulfur, which could affect the local environment of the framework. Moreover, S-CTF-1 also exhibited dominant signals at 464, 234, and 162 cm^{-1}. While the peak at 464 cm^{-1} corresponds to S–S stretching, the peaks at 234 and 162 cm^{-1} were assigned to C–S stretching.[21] The molecular connectivity of S-CTF-1 was also investigated by solid-state CP/MAS ^{13}C NMR spectroscopy (Figure 1f). The CP/MAS ^{13}C NMR spectrum of S-CTF-1 showed a broad signal between 120–150 ppm and a small resonance at 170 ppm. The signal at 170 ppm was assigned to the carbon atoms in the triazine ring,[15d,22] whereas the resonance at 120–150 ppm corresponds to the aryl rings bonded to the triazine rings and sulfur.[21] Thermogravimetric analysis (TGA) of S-CTF-1 showed a weight loss that started at 150 °C, which is due to the presence of elemental sulfur within the pores, and continued to 300 °C (Figure S3). The weight loss consistently indicates the sulfur content of S-CTF-1 to be approximately 60 wt %.

The morphology of S-CTF-1 was characterized by field emission scanning electron microscopy (FE-SEM) and transmission electron microscopy (TEM), which revealed a uniform bipyramidal shape morphology even though neither an external template nor a structure-directing agent had been used (Figure 2a, b).[17] It is anticipated that the in situ generated covalent triazine framework acts as a structural template for the accumulation of crystalline sulfur particles, which enables the formation of this well-defined superstructure, although further investigations are needed for an in-depth understanding of the mechanism. Elemental maps of S-CTF-1 were obtained by energy-dispersive X-ray (EDAX) analysis (Figure 2c–f) and indicate the homogeneous distribution of carbon, sulfur, and nitrogen throughout the sample.

To test the electrochemical properties of S-CTF-1, galvanostatic measurements using CR2032 half cells were carried out. The electrode was fabricated using S-CTF-1 (active material), PVDF (binder), and super P (conductive agent) in a mass ratio of 60:10:30 by the doctor-blade method. Li metal discs were used as counter and reference electrodes. 1 M LiTFSI in tetraethylene glycol dimethyl ether/1,3-dioxolane (TEGDME/DIOX = 0.33:0.67) was used as the electrolyte, and 0.2 M $LiNO_3$ was added to protect the surface of the Li metal.[23] The voltage range was set to 1.7–2.7 V vs. Li/Li^+ in all electrochemical tests. The current densities for electrochemical characterization were calculated based on the

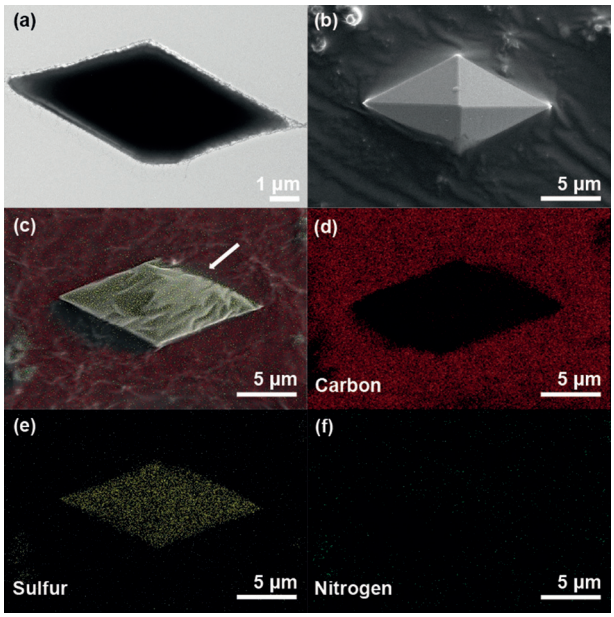

Figure 2. a) TEM and b) SEM images of a single S-CTF-1 particle. c–f) EDS elemental maps for carbon (d), sulfur (e), nitrogen (f), and all elements combined (c).

weight of the whole active material, and all potentials hereafter are with respect to Li/Li^+ (in V). The first discharge–charge voltage profiles of S-CTF-1 were attained at 0.05 C (Figures 3a and S4). Consistent with the previously reported S_8 cases,[1b,3–4,7] the profiles exhibited two plateaus; the discharge curve corresponds to a two-step reduction process that includes the formation of Li polysulfide species (Li_2S_n, $n \geq 4$) at 2.35 V and lithium sulfide (Li_2S) at 2.1 V as the final discharge product. During charging, the crystalline Li_2S is oxidized to Li polysulfide species at 2.3 V and then to sulfur at 2.4 V as the final charge product. The initial discharge/charge capacities were 670 mAh g^{-1} and 632 mAh g^{-1}, leading to an exceptional ICE of 94.4%. This ICE value is remarkable, as it is higher than those of any other organic-based matrix/sulfur composite and S_8-encapsulated cathodes.[3–9] The high ICE implies that our framework is well-organized with negligible defects and dangling groups, and the electrode forms a stable interface with the electrolyte without serious shuttling problems.[1b,3] Obviously, this high ICE is very important for the cell energy density because a smaller excess of cathode material is required for n/p balancing in the initial cell design.

More importantly, S-CTF-1 showed stable cycling performance (Figure 3b): After 50 cycles, 84.3% capacity retention and 99.7% Coulombic efficiency were recorded at 0.2 C. A control electrode was prepared by simple mechanical mixing of sulfur and Ketjen Black (in a mass ratio of 50:50 by thermal annealing at 150 °C for 12 h, KB-S). However, under the same measurement conditions, even after only 25 cycles, KB-S showed only 69.3% capacity retention and 99.5% Coulombic efficiency. When tested at 1 C and 2 C for prolonged cycling, S-CTF-1 retained 85.8% and 81.0%, respectively, of the initial capacities (482.2 and 406.3 mAh g^{-1}) after 300 cycles (Figure 3c). At 1 C, the CE rose quickly from 94.4% in the first cycle to 98.0, 99.9, 99.9, 100.0, 100.0, and 100.1% in the 2nd, 5th, 10th, 30th, 100th, and 300th cycle, respectively, corroborating the stability of the solid–electrolyte interface of the S-CTF-1 electrode. At 2 C, the CEs were 94.4, 98.0, 99.6, 99.8, 100.0, 100.0, and 100.1%, respectively, for the same cycle

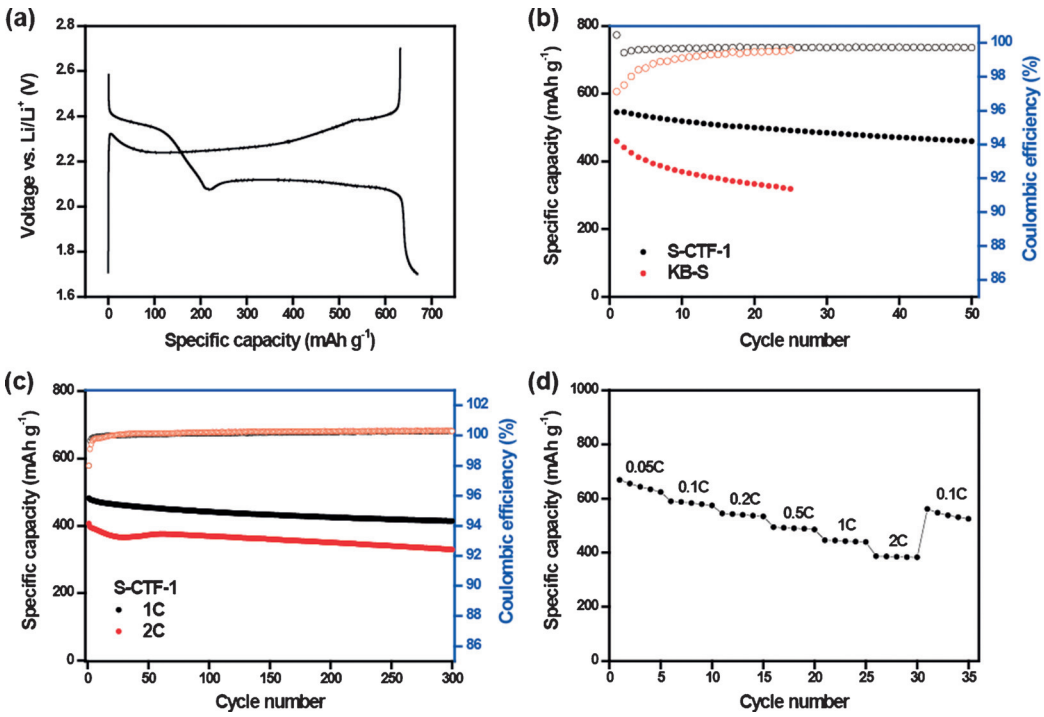

Figure 3. Electrochemical performance of S-CTF-1. a) First discharge and charge curves of S-CTF-1 measured at 0.05 C. b) Cycling performance and CEs of S-CTF-1 in comparison with a control sample, KB-S. The tests were performed at 0.2 C. c) Cycling performance of S-CTF-1 measured at 1 C and 2 C. d) Rate performance of S-CTF-1 measured at various C rates. The C rates for both discharge and charge were the same in each cycle. The specific capacities were calculated with respect to the total weight of the active material, and the absolute areal sulfur loading was 0.50 mg cm^{-2}.

numbers. This stable cycling performance is due to the robust sulfur cathode structure in which sulfur is homogeneously distributed throughout the regular micropores within the

triazine-based framework together with the C–S covalent links. The effect of robust C–S bonds was confirmed by ex situ XPS analysis of the electrodes. The XPS S 2p, N 1s, and Li 1s profiles of the electrodes after the 1st, 2nd, and 20th cycle (Figure S5) clearly demonstrate the reversibility of the discharge and charge processes in each cycle. Importantly, after discharge in each cycle, a peak shift to higher binding energies was observed for the S 2p band of S-CTF-1 compared to the pristine sample, indicating the reversible formation of Li polysulfides within the framework. More significantly, the N 1s peak at 405 eV that appears after discharge provides us with clear evidence for the interaction of the triazine nitrogen atoms with the lithium ions, thus stabilizing the lithium polysulfides without their severe dissolution. Moreover, XPS S 2p analysis after 100 cycles (Figure S6) clearly demonstrates the robustness of C–S bonds within the framework structure. S-CTF-1 also exhibited an excellent rate performance (Figures 3 d and S4), as it preserved 90.6, 83.9, 76.1, 68.7, and 59.8 % of the original capacity (670 mAh g^{-1}) with a C rate increase from 0.05 C to 0.1, 0.2, 0.5, 1, and 2 C, respectively. We attribute this superior rate capability to the well-defined sulfur distribution within the micropores of CTF-1 as well as the conductive nature of the framework.

In conclusion, we have described the catalyst- and solvent-free synthesis of CTFs in the presence of elemental sulfur for the first time. In situ formation of the framework structure and chemical impregnation of sulfur not only led to a homogeneous sulfur distribution, but also enabled a high sulfur content of 62 wt %. S-CTF-1 was shown to be an excellent cathode material for Li–S batteries with superior ICEs and cycle lifetimes as it benefits from the formation of well-confined sulfur species within the micropores, sulfur bonding with the framework, and the good electron and ion conductivity of the framework. Our results demonstrate the promising properties of microporous polymers as active supports for sulfur, which is expected to motivate further research in this area. In a broader perspective, the direct utilization of elemental sulfur for the synthesis of covalent triazine frameworks can enable new high-value applications, such as advanced electrode materials for energy storage and conversion.

Acknowledgements

We acknowledge support from the Basic Science Research Program through the National Research Foundation of Korea (NRF), which is funded by the Ministry of Science, ICT & Future Planning (NRF-2012-R1A2A1A01011970, 2013R1A1A1012282). This work was supported by the Energy Efficiency & Resources Core Technology Program of the Korea Institute of Energy Technology Evaluation and Planning (KETEP), which is granted financial resources from the Ministry of Trade, Industry & Energy, Republic of Korea (20152020104870). This work was also partially supported by a National Research Foundation of Korea (NRF) Grant funded by the Korea government (MEST; NRF-2014R1A4A1003712) and the BK21 PLUS program.

Keywords: cathode materials · electrochemistry · lithium–sulfur batteries · microporous materials · sulfur

How to cite: *Angew. Chem. Int. Ed.* **2016**, *55*, 3106–3111
Angew. Chem. **2016**, *128*, 3158–3163

[1] a) D. Peramunage, S. Licht, *Science* **1993**, *261*, 1029–1032; b) A. Manthiram, Y. Fu, S. H. Chung, C. Zu, Y. S. Su, *Chem. Rev.* **2014**, *114*, 11751–11787.
[2] a) Y. V. Mikhaylik, J. R. Akridge, *J. Electrochem. Soc.* **2004**, *151*, A1969–A1976; b) B. L. Ellis, K. T. Lee, L. F. Nazar, *Chem. Mater.* **2010**, *22*, 691–714; c) C. Barchasz, J. C. Lepretre, F. Alloin, S. Patoux, *J. Power Sources* **2012**, *199*, 322–330; d) M. K. Song, E. J. Cairns, Y. Zhang, *Nanoscale* **2013**, *5*, 2186–2204.
[3] X. Ji, K. T. Lee, L. F. Nazar, *Nat. Mater.* **2009**, *8*, 500–506.
[4] a) D. S. Jung, T. H. Hwang, J. H. Lee, H. Y. Koo, R. A. Shakoor, R. Kahraman, Y. N. Jo, M.-S. Park, J. W. Choi, *Nano Lett.* **2014**, *14*, 4418–4425; b) C. Zhang, H. B. Wu, C. Yuan, Z. Guo, X. W. Lou, *Angew. Chem. Int. Ed.* **2012**, *51*, 9592–9595; *Angew. Chem.* **2012**, *124*, 9730–9733.
[5] a) J. Guo, Y. Xu, C. Wang, *Nano Lett.* **2011**, *11*, 4288–4294; b) T. Xu, J. Song, M. L. Gordin, H. Sohn, Z. Yu, S. Chen, D. Wang, *ACS Appl. Mater. Interfaces* **2013**, *5*, 11355–11362.
[6] L. Ji, M. Rao, S. Aloni, L. Wang, E. J. Cairns, Y. Zhang, *Energy Environ. Sci.* **2011**, *4*, 5053–5059.
[7] H. Wang, Y. Yang, Y. Liang, J. T. Robinson, Y. Li, A. Jackson, Y. Cui, H. Dai, *Nano Lett.* **2011**, *11*, 2644–2647.
[8] Y. Yang, G. Yu, J. J. Cha, H. Wu, M. Vosgueritchian, Y. Yao, Z. Bao, Y. Cui, *ACS Nano* **2011**, *5*, 9187–9193.
[9] a) J. Wang, J. Yang, C. Wan, K. Du, J. Xie, N. Xu, *Adv. Funct. Mater.* **2003**, *13*, 487–492; b) S. Wei, L. Ma, K. E. Hendrickson, Z. Tu, L. A. Archer, *J. Am. Chem. Soc.* **2015**, *137*, 12143–12152; c) J.-S. Kim, T. H. Hwang, B. G. Kim, J. Min, J. W. Choi, *Adv. Funct. Mater.* **2014**, *24*, 5359–5367.
[10] a) S. Evers, T. Yim, L. F. Nazar, *J. Phys. Chem. C* **2012**, *116*, 19653–19658; b) H. Kim, J. T. Lee, D.-C. Lee, A. Magasinski, W.-i. Cho, G. Yushin, *Adv. Energy Mater.* **2013**, *3*, 1308–1315; c) Z. Wei Seh, W. Li, J. J. Cha, G. Zheng, Y. Yang, M. T. McDowell, P.-C. Hsu, Y. Cui, *Nat. Commun.* **2013**, *4*, 1331.
[11] a) G. Zheng, Q. Zhang, J. J. Cha, Y. Yang, W. Li, Z. W. Seh, Y. Cui, *Nano Lett.* **2013**, *13*, 1265–1270; b) W. Zhou, X. Xiao, M. Cai, L. Yang, *Nano Lett.* **2014**, *14*, 5250–5256; c) S. Zheng, F. Yi, Z. Li, Y. Zhu, Y. Xu, C. Luo, J. Yang, C. Wang, *Adv. Funct. Mater.* **2014**, *24*, 4156–4163.
[12] a) A. G. Simmonds, J. J. Griebel, J. Park, K. R. Kim, W. J. Chung, V. P. Oleshko, J. Kim, E. T. Kim, R. S. Glass, C. L. Soles, Y.-E. Sung, K. Char, J. Pyun, *ACS Macro Lett.* **2014**, *3*, 229–232; b) W. J. Chung, J. J. Griebel, E. T. Kim, H. Yoon, A. G. Simmonds, H. J. Ji, P. T. Dirlam, R. S. Glass, J. J. Wie, N. A. Nguyen, B. W. Guralnick, J. Park, S. Árpád, P. Theato, M. E. Mackay, Y.-E. Sung, K. Char, J. Pyun, *Nat. Chem.* **2013**, *5*, 518–524.
[13] H. Kim, J. Lee, H. Ahn, O. Kim, M. J. Park, *Nat. Commun.* **2015**, *6*, 7278.
[14] P. Kuhn, M. Antonietti, A. Thomas, *Angew. Chem. Int. Ed.* **2008**, *47*, 3450–3453; *Angew. Chem.* **2008**, *120*, 3499–3502.
[15] a) R. Palkovits, M. Antonietti, P. Kuhn, A. Thomas, F. Schüth, *Angew. Chem. Int. Ed.* **2009**, *48*, 6909–6912; *Angew. Chem.* **2009**, *121*, 7042–7045; b) C. E. Chan-Thaw, A. Villa, P. Katekomol, D. Su, A. Thomas, L. Prati, *Nano Lett.* **2010**, *10*, 537–541; c) P. Katekomol, J. Roeser, M. Bojdys, J. Weber, A. Thomas, *Chem. Mater.* **2013**, *25*, 1542–1548; d) K. Schwinghammer, S. Hug, M. B. Mesch, J. Senker, B. V. Lotsch, *Energy Environ. Sci.* **2015**, *8*, 3345–3353; e) L.-M. Tao, F. Niu, D. Zhang, T.-M. Wang, Q.-H. Wang, *New J. Chem.* **2014**, *38*, 2774–2777; f) H. Ren, T. Ben, E. Wang, X. Jing, M. Xue, B. Liu, Y. Cui, S. Qiu, G. Zhu, *Chem. Commun.* **2010**, *46*, 291–293; g) H. Ma, H. Ren, S. Meng,

F. Sun, G. Zhu, *Sci. Rep.* **2013**, *3*, 2611; h) L. Hao, J. Ning, B. Luo, B. Wang, Y. Zhang, Z. Tang, J. Yang, A. Thomas, L. Zhi, *J. Am. Chem. Soc.* **2015**, *137*, 219 – 225; i) L. Hao, S. Zhang, R. Liu, J. Ning, G. Zhang, L. Zhi, *Adv. Mater.* **2015**, *27*, 3190 – 3195; j) K. A. See, S. Hug, K. Schwinghammer, M. A. Lumley, Y. Zheng, J. M. Nolt, G. D. Stucky, F. Wudl, B. V. Lotsch, R. Seshadri, *Chem. Mater.* **2015**, *27*, 3821 – 3829; k) K. Iwase, T. Yoshioka, S. Nakanishi, K. Hashimoto, K. Kamiya, *Angew. Chem. Int. Ed.* **2015**, *54*, 11068 – 11072; *Angew. Chem.* **2015**, *127*, 11220 – 11224; l) Y. Su, Y. Liu, P. Liu, D. Wu, X. Zhuang, F. Zhang, X. Feng, *Angew. Chem. Int. Ed.* **2015**, *54*, 1812 – 1816; *Angew. Chem.* **2015**, *127*, 1832 – 1836.

[16] a) X. Zhu, C. Tian, S. M. Mahurin, S.-H. Chai, C. Wang, S. Brown, G. M. Veith, H. Luo, H. Liu, S. Dai, *J. Am. Chem. Soc.* **2012**, *134*, 10478 – 10484; b) S. Ren, M. J. Bojdys, R. Dawson, A. Laybourn, Y. Z. Khimyak, D. J. Adams, A. I. Cooper, *Adv. Mater.* **2012**, *24*, 2357 – 2361.

[17] Y. Fu, A. Manthiram, *J. Phys. Chem. C* **2012**, *116*, 8910 – 8915.

[18] a) D. Sun, J. Yang, X. Yan, *Chem. Commun.* **2015**, *51*, 2134 – 2137; b) W. Li, M. Zhou, H. Li, K. Wang, S. Cheng, K. Jiang, *Energy Environ. Sci.* **2015**, *8*, 2916 – 2921.

[19] W. J. Gammon, O. Kraft, A. C. Reilly, B. C. Holloway, *Carbon* **2003**, *41*, 1917 – 1923.

[20] a) S. Yang, L. Zhi, K. Tang, X. Feng, J. Maier, K. Müllen, *Adv. Funct. Mater.* **2012**, *22*, 3634 – 3640; b) L. Xiao, Y. Cao, J. Xiao, B. Schwenzer, M. H. Engelhard, L. V. Saraf, Z. Nie, G. J. Exarhos, J. Liu, *Adv. Mater.* **2012**, *24*, 1176 – 1181.

[21] M. P. Crockett, A. M. Evans, M. J. H. Worthington, I. S. Albuquerque, A. D. Slattery, C. T. Gibson, J. A. Campbell, D. A. Lewis, G. J. L. Bernardes, J. M. Chalker, *Angew. Chem. Int. Ed.* **2016**, *55*, 1714 – 1718; *Angew. Chem.* **2016**, *128*, 1746 – 1750.

[22] B. Jürgens, E. Irran, J. Senker, P. Kroll, H. Müller, W. Schnick, *J. Am. Chem. Soc.* **2003**, *125*, 10288 – 10300.

[23] D. Aurbach, E. Pollak, R. Elazari, G. Salitra, C. S. Kelley, J. Affinito, *J. Electrochem. Soc.* **2009**, *156*, A694 – A702.

Received: December 12, 2015
Revised: December 29, 2015
Published online: January 28, 2016

